

See discussions, stats, and author profiles for this publication at: <https://www.researchgate.net/publication/46887954>

# CLPH, a Novel Casein Kinase 2-Phosphorylated Disordered Protein, Is Specifically Associated with Postmeiotic Germ Cells in Rat Spermatogenesis

ARTICLE *in* JOURNAL OF PROTEOME RESEARCH · JUNE 2009

Impact Factor: 4.25 · DOI: 10.1021/pr900082m · Source: OAI

---

CITATIONS

7

READS

15

## 9 AUTHORS, INCLUDING:



Pierre Calvel

Institut Pasteur International Network

20 PUBLICATIONS 196 CITATIONS

[SEE PROFILE](#)



Antoine D Rolland

Université de Rennes 1

36 PUBLICATIONS 514 CITATIONS

[SEE PROFILE](#)



Frederic Chalmel

French Institute of Health and Medical Res...

57 PUBLICATIONS 1,501 CITATIONS

[SEE PROFILE](#)



Charles Pineau

French Institute of Health and Medical Res...

125 PUBLICATIONS 1,907 CITATIONS

[SEE PROFILE](#)

## CLPH, a Novel Casein Kinase 2-Phosphorylated Disordered Protein, Is Specifically Associated with Postmeiotic Germ Cells in Rat Spermatogenesis

Pierre Calvel,<sup>†,‡</sup> Christine Kervarrec,<sup>†,‡</sup> Régis Lavigne,<sup>§</sup> Virginie Vallet-Erdtmann,<sup>†,‡</sup> Myriam Guerrois,<sup>†,‡</sup> Antoine D. Rolland,<sup>†,‡</sup> Frédéric Chalmel,<sup>†,‡</sup> Bernard Jégou,<sup>†,‡</sup> and Charles Pineau<sup>\*,†,‡,§</sup>

Inserm, U625, Rennes, France, Université Rennes I, Campus de Beaulieu, IFR-140, GERHM, Rennes, F-35042, France, and Proteomics Core Facility OUEST-genopole, Campus de Beaulieu, Rennes cedex, F-35042 France

Received February 2, 2009

In a recent proteomic study of rat spermatogenesis, we identified CLPH (for Casein-Like PHosphoprotein), a new testis-specific protein expressed exclusively in postmeiotic germ cells. *In situ* hybridization showed that the CLPH transcript was mainly present in round spermatids, whereas the protein was specifically detected by immunohistochemistry in elongated spermatids and in residual bodies. Electron microscopy showed the protein to be mostly cytoplasmic, but also frequently associated with the mitochondrial inner membrane during the last steps of spermatid differentiation. The *Ciph* gene was found to be present solely in mammalian genomes, in a chromosomal region syntenic to the mammalian cluster of secretory calcium-binding phosphoprotein (SCPP) genes. CLPH has several distinctive properties in common with SCPPs: calcium overlay experiments showed that CLPH was a calcium-binding protein, whereas trypsin digestion assay, circular dichroism and fluorescence experiments demonstrated its intrinsically disordered structure. We also showed that CLPH was phosphorylated *in vitro* and *in vivo* by casein kinase 2, an enzyme critical for spermatid elongation. Given the specific and strong production of CLPH during rat spermiogenesis, together with the particular biochemical properties of this protein, we suggest that CLPH is involved in the extremely complex structural rearrangements occurring in haploid germ cells during spermiogenesis.

**Keywords:** testis • spermatids • SCPP • Casein Kinase 2 • calcium-binding • intrinsic disorder

### Introduction

Spermatogenesis is a sophisticated process facilitating transmission of the genetic patrimony and, thus, perpetuation of the species. Mammalian spermatogenesis is classically divided into three phases. In the first—the proliferative or mitotic phase—primitive germ cells or spermatogonia undergo a series of mitotic divisions. In the second—the meiotic phase—the spermatocytes undergo two consecutive divisions to produce the haploid spermatids. In the third—the postmeiotic phase—spermatids differentiate into spermatozoa. This last step, also known as spermiogenesis, is a striking and unique example of cell differentiation involving acrosome formation, nuclear condensation and flagellum biogenesis. The entire process of spermatogenesis is regulated by paracrine, autocrine and endocrine pathways, an array of structural elements and

chemical factors modulating somatic and germ cell activity (for reviews, see refs 1–6).

The advances in molecular biology and genomics made over the last 20 years have greatly improved our overall understanding of spermatogenesis, by identifying a number of genes essential for the development of functional male gametes (for reviews, see refs 7 and 8). Indeed, several laboratories have built on rapid progress in genome sequencing and microarray analysis, by carrying out genome-wide expression studies, leading to the identification of hundreds of genes differentially expressed within the testis (for review, see ref 9). Similarly, advances in the development of tools for high-throughput protein identification have enabled a few laboratories to undertake differential protein profiling expression studies and/or the systematic analysis of testicular proteomes from various species. These proteomic studies, based either on the entire organ<sup>10,11</sup> or on isolated cells,<sup>12,13</sup> have provided a comprehensive view of the translational and post-translational regulations operating during male germ cell differentiation. However, despite the significant contribution of these extensive studies to our global knowledge of male germ cell fate in the form of a precise timetable of the production of many well character-

\* Corresponding author: Charles Pineau, INSERM, U625, GERHM, Campus de Beaulieu, University of Rennes I, 35042 Rennes cedex, France, Tel: +33(0)2 2323 5072; Fax: +33(0)2 2323 5055. E-mail: charles.pineau@rennes.inserm.fr.

<sup>†</sup> Inserm, U625.

<sup>‡</sup> Université Rennes I, Campus de Beaulieu.

<sup>§</sup> Proteomics Core Facility OUEST-genopole, Campus de Beaulieu.

ized testicular factors, the roles of many testis-specific transcripts and proteins remain totally unknown.

We report here the first analysis and characterization of CLPH, a new testis-specific protein identified by a two-dimensional fluorescence difference gel electrophoresis (2D-DIGE) comparison of male germ cells at different stages of differentiation.<sup>13</sup> This previously unknown protein displayed strong variation in relative expression levels during spermatogenesis and was shown to be spermatid-specific in this previous study. Searches of databases and published studies provided no link between CLPH and an existing molecular function, suggesting a putative unknown element of the rat spermatogenesis regulation network, localized and characterized for the first time here.

## Experimental Procedures

**Animals and Reagents.** Male Sprague–Dawley rats of various ages were used for tissue collection, testicular cell isolation, *in situ* hybridization and immunohistochemical experiments. They were purchased from Elevage Janvier (Le Genest-Saint-Isle, France).

**Isolation of Testicular Cell.** Early spermatids were prepared from adult rat testes, by mechanical disruption followed by centrifugal elutriation, giving an 85–90% pure preparation.<sup>14</sup> Cells were gently pelleted, snap-frozen in liquid nitrogen and stored at –80 °C for the extraction of RNA and protein.

**Protein Extraction.** Cell pellets were resuspended in 3 vol of ice-cold 20 mM HEPES lysis buffer pH 7.5 supplemented with Protease Inhibitor Mix (GE Healthcare, Orsay, France) according to the manufacturer's instructions. Cell suspensions were homogenized by sonication on ice and centrifuged at 15 000g for 30 min at 4 °C. Supernatants were ultracentrifuged at 105 000g for 1 h at 4 °C. Proteins were extracted from various rat tissues, using the protocol described above, but with an initial step involving mechanical disruption for 10 min in lysis buffer, with a Teflon pestle. The protein concentration of the resulting supernatants was determined by the bicinchoninic acid assay (Sigma-Aldrich, Saint-Quentin Fallavier, France) according to the manufacturer's instructions.

**Two-Dimensional Electrophoresis.** Spermatid protein extract (150 µg of protein) was incubated with a rehydration buffer containing 6 M urea, 2 M thiourea, 1% DTT, 4% CHAPS, 0.5% IPG Buffer (GE Healthcare), and bromophenol blue, for 1 h, at room temperature. Two-dimensional electrophoresis (2DE) was then carried out as previously described.<sup>12</sup>

**Protein Identification by Mass Spectrometry.** Silver-stained protein spots were manually excised from the 2-D gel and processed for trypsic digestion, as previously described.<sup>13</sup> Mass fingerprints were acquired with a MALDI-TOF/TOF mass spectrometer (Ultraflex; Bruker Daltonik, GmbH, Bremen, Germany) and processed with FlexAnalysis software (version 2.2; Bruker Daltonik, GmbH). After internal calibration with trypsin autodigestion peptides, the monoisotopic masses of tryptic peptides were used to query NCBI sequence databases (version 20060609, 3 682 060 sequences), using the Mascot search algorithm (Mascot server version 2.1.04; <http://www.matrixscience.com>). Each identification was carefully checked, as previously described,<sup>12</sup> to ensure that identification was unambiguous.

**In Silico Analysis of CLPH Nucleotide and Peptide Sequences.** For the identification of putative orthologs of the *Clph* genes, we mapped the rat gene (Rat interim symbol: *Rsd6* – NC\_005113.2) and protein (NP\_071559.2) against all the avail-

able vertebrate genomes in the UCSC genome browser Web site and Ensembl blastview.<sup>15,16</sup> Prosite and Pfam databases were used to identify potential structural domains in the rat protein.<sup>17,18</sup> The research for known protein sequence motifs was carried out using the Scansite Web tool,<sup>19</sup> with a high stringency level of analysis. Amino acid sequence conservation was evaluated with the ClustalW multiple alignment program.<sup>20</sup> Finally, disordered domains were predicted with the FoldIndex Web tool,<sup>21</sup> using an analysis window of 20 residues and a step analysis set to 5 residues. All other programs were used with default parameter settings.

**RT-PCR and Cloning of the Rat *Clph* Gene.** An RT-PCR-based strategy was used to amplify the full-length CLPH cDNA from rat testis for insertion into PQE30 (Qiagen, Courtaboeuf, France) or pBluescript KS (-) (Fermentas, St. Leon-Rot, Germany), according to the manufacturer's instructions. The following primers were used: forward (5'CGCGGATCCGCT-GAAGATGGATCTCCC3'-*Bam*H) and reverse (5'CGGGGTAC-CCATCATGAGTTCATCTGG3'-*Kpn*I). The integrity, insertion and orientation of the CLPH cDNA in the vectors were checked by sequencing, using the PRISM Ampli-Taq FS Big Dye Terminator kit (Applied Biosystems, Courtaboeuf, France).

CLPH transcript levels were investigated by carrying out PCR on total cDNA preparations from various organs, with the following primers: forward: (5'GAAGTCAAACCCACTACTGAGC) and reverse (5'CAGCTGGCTCCTCATCAGTT3').

**Riboprobe Synthesis and *in Situ* Hybridization.** Digoxigenin (DIG)-labeled RNA probes were synthesized from pBluescript II KS (-) vectors containing the CLPH cDNA, using the Riboprobe Combination system-T3/T7 RNA polymerase (Promega, Charbonnières-les-bains, France), according to the manufacturer's instructions. *In situ* hybridization experiments were carried out on 5 µm sections of paraffin-embedded Bouin fixative-perfused adult rat testis. Sections were rehydrated and incubated for 40 min at 37 °C with 3 µg/mL Proteinase K (Eurobio, Courtaboeuf, France). They were then washed in successive baths of 0.2% glycine, triethanolamine-HCl buffer and Tris-EDTA-saline buffer and coated by incubation for 3 h at 37 °C in hybridization buffer containing 120 µg/mL of salmon testes DNA and 120 µg/mL of yeast tRNA. Sections were then incubated overnight at 37 °C with 25 ng of DIG-labeled CLPH antisense or sense probes diluted in hybridization buffer supplemented with 0.1 g/mL dextran sulfate. The sections were then processed as previously described.<sup>22</sup> The hybridization signal was detected with an alkaline phosphatase-conjugated anti-DIG antibody (Roche, Meylan, France) and visualized by incubation with nitroblue tetrazolium/bromochlorylindolophosphate chromogen.

**Production of Recombinant CLPH Protein.** XL1blue strain supercompetent bacteria (Stratagene, Amsterdam, The Netherlands) transformed with the PQE30 vector containing the CLPH cDNA were cultured in Luria Broth (LB) supplemented with ampicillin (100 µg/mL) and isopropyl β-D-1-thiogalactopyranoside (IPTG, 0.6 mM) to induce recombinant protein production. After bacteria lysis, the soluble HIS-tagged recombinant CLPH (<sub>rec</sub>CLPH) present in the supernatant was purified on Ni-NTA agarose resin (Qiagen), according to the manufacturer's instructions. <sub>rec</sub>CLPH-containing fractions were further enriched and desalts by reversed phase high-performance liquid chromatography (RP-HPLC), lyophilized and resuspended in 20 mM sodium phosphate buffer, pH 7.2. Small aliquots of <sub>rec</sub>CLPH were subjected to SDS-PAGE onto a 10% acrylamide gel, to evaluate the purity of the preparation. The

nature of the recombinant protein was investigated by in-gel trypsic digestion, peptide mass fingerprinting and MS/MS.

**Chemical Modification of Glutamic Acid and Aspartic Acid Residues.** Modification of *rec*CLPH was carried out following a previously described protocol.<sup>23</sup> Briefly, 10 µg of *rec*CLPH were incubated with carbodiimide 12 mM/ethanolamine 500 mM in 30 mM MES buffer for 2 h and resolved onto a 10% SDS-PAGE gel.

**Antibody.** Antibodies against *rec*CLPH were raised in rabbit, using the “28-day Super Speedy Polyclonal Antibody Protocol” (Eurogentec, Angers, France). Specificity for the endogenous CLPH protein was assessed by two-dimensional Western blotting on rat total testis protein extracts, followed by trypsin digestion and peptide mass fingerprinting.

**Western Blot Analysis.** Protein samples (20 µg of protein) were separated by SDS-PAGE onto 10% polyacrylamide gels and the resulting bands were transferred onto polyvinylidene difluoride (PVDF) Immobilon-P<sup>SQ</sup> membranes (Millipore, Molsheim, France). Blots were probed with the anti-rat CLPH antibody at a dilution of 1:40 000. Immune complexes were detected with a horseradish peroxidase-conjugated secondary goat anti-rabbit antibody (GE Healthcare) and the ECL+ Detection System (GE Healthcare).

**Immunolocalization of the CLPH Protein.** Immunohistochemical experiments were performed on testes from 90 dpp male Sprague–Dawley rats fixed in Bouin’s fixative and embedded in paraffin, as previously described.<sup>24</sup> The antibody against CLPH and preimmune serum were used at a working dilution of 1:10 000.

**Electron Microscopy.** Immunogold electron microscopy and appropriate controls were carried out on adult rat testes following a previously described protocol<sup>25</sup> with modifications. Briefly, testes were fixed by immersion in paraformaldehyde (2%) and glutaraldehyde (0.2%) in phosphate buffer (0.1 M, pH 7.4), dehydrated in ethanol and embedded in LRWhite resin (London Resin Company, Theale, England). Ultrathin sections (70 nm) were placed on 200 mesh Formvar-coated nickel grids and incubated with 5% BSA in a blocking buffer (Aurion BSA-c, Aurion, Wageningen, The Netherlands). The grids were incubated overnight at 4 °C with either rabbit anti-CLPH antibody (1:1000) or rabbit preimmune serum (1:1000) in the blocking solution, washed with 0.1% BSA in PBS, incubated with colloidal gold-labeled (10 nm) secondary goat anti-rabbit antibody (1:50) (Aurion, Wageningen, The Netherlands) and counterstained with 4% uranyl acetate. Sections were observed with a CM10 electron microscope (Philips, Eindhoven, Netherlands). Images were acquired with the Solf Imaging System (Germany).

#### Immunoprecipitation of CLPH from Spermatid Protein Extracts.

Native CLPH was immunoprecipitated from spermatid protein extracts using our anti-CLPH antibody and a Dynabeads Protein A kit (Invitrogen, Cergy Pontoise, France), according to the manufacturer’s instructions. Preimmune serum was used as a negative control. Immunocomplexes were eluted in Laemmli buffer, boiled for 5 min and resolved by SDS-PAGE onto a 10% acrylamide gel. Gel Coomassie blue staining was preferred to silver staining to avoid artifactual sulfation of hydroxylated amino acid residues.<sup>26</sup> Stained protein bands were sliced off the gel and digested with trypsin, as previously described,<sup>13</sup> for nano-LC-MS/MS analysis.

**Phosphopeptide Analysis by Nano-LC-MS/MS.** CLPH digestion peptides were separated by nanoflow reversed phase liquid chromatography and analyzed with an HCT Ultra PTM Dis-

covery (Bruker Daltonik, GmbH) ion trap mass spectrometer equipped with electrospray ionization (ESI). Precolumn was a 5 mm × 300 µm i.d., 300 Å pore size, Pepmap C18, 5 µm (Dionex, LC Packings, Amsterdam, The Netherlands). Analytical column was a 15 cm × 300 µm i.d., 300 Å pore size, Pepmap C18, 5 µm (Dionex, LC Packings). Mobile phases A (0.05% formic acid in water) and B (0.05% formic acid in acetonitrile) were delivered by an Ultimate 3000 nanoflow LC system (Dionex, LC Packings). Trypsin digests loaded onto the pre-column were eluted with a linear gradient of 2–90% solvent B, at a flow rate of 250 nL/min for 75 min. The mass spectrometer was operated in a data-dependent mode, permitting automatic switching between MS and MS<sup>2</sup> for collision-induced dissociation (CID) fragmentation. The raw MS<sup>2</sup> data were searched using Mascot (version 2.2; Matrix Science Ltd, London, U.K.) and Phenix (version 2.5; Genebio, Geneva, Switzerland) on a Linux 12-node parallel virtual machine cluster computer, against the NCBI protein sequence database (version 20080718, 6 833 826 sequences). A peptide mass tolerance of 1 Da for MS data and a fragment ion tolerance of 0.5 Da were allowed, with a trypsin specificity of one missed cleavage allowed. Oxydation (M) and carbamidomethylation (C) were selected as fixed modifications, whereas phosphorylation (STY) was set as variable modification. Manual inspection of all MS<sup>2</sup> spectra for modified peptides was performed to validate assignments.

**Phosphorylation of Recombinant CLPH Protein by Casein Kinase 2.** *rec*CLPH protein (10 µg) was phosphorylated by incubation with 0.012 units of rat recombinant casein kinase 2 catalytic subunits (Sigma) in 50 µL of phosphorylation buffer [80 mM HEPES, 10 mM MgCl<sub>2</sub>, 5 mM DTT, 130 mM KCl, pH 7.5] supplemented with 0.1 mM ATP at 37 °C for 15 min. *rec*CLPH phosphorylation was monitored by including trace amounts (2 µCi) of [ $\gamma$ -<sup>32</sup>P] ATP (Perkin-Elmer, Courtaboeuf, France) in the reaction. The incorporation of [<sup>32</sup>P]-phosphate was followed by SDS-PAGE and autoradiography. Heparin, a competitive inhibitor of casein kinase 2, was added to the mixture (10 µg/mL) as a reaction control. Bovine caseins (10 µg; Sigma) or BSA were processed in the same way as positive and negative controls, respectively. One microgram of phosphorylated or unmodified *rec*CLPH was reduced by a DTT/iodoacetamide treatment (65 mM/135 mM, 15 min each), then submitted to digestion by porcine trypsin (100 ng, 4 h) before analysis by nano-LC-MS/MS, under conditions identical to those described for the native CLPH.

**Calcium Binding Assay.** We investigated the binding of the *rec*CLPH protein to <sup>45</sup>Ca<sup>2+</sup>, using a protocol described elsewhere.<sup>27</sup> BSA and bovine caseins were used as negative and positive controls of <sup>45</sup>Ca<sup>2+</sup> binding, respectively.

**Tryptic Digestion of CLPH.** Tryptic digestions of *rec*CLPH and BSA were carried out according a modified version of a protocol described elsewhere.<sup>28</sup> Briefly, 10 µg of *rec*CLPH or BSA was mixed with various dilutions of trypsin (Promega, Charbonnières-les-bains, France) in 100 mM ammonium bicarbonate, to obtain the following final trypsin/substrate ratios: 1/400, 1/800, 1/1600, 1/3200, 1/6400. Mixtures were then incubated for 30 min at 37 °C. The reaction was stopped by adding 4× Laemmli sample buffer and incubating for 5 min at 100 °C. The digests were resolved by SDS-PAGE in a 15% polyacrylamide gel.

**Circular Dichroism.** Circular dichroism spectra were generated with the CD6 dichrograph (Horiba Jobin Yvon, Villeneuve d’Ascq, France). Spectra were an average of 10 accumulated

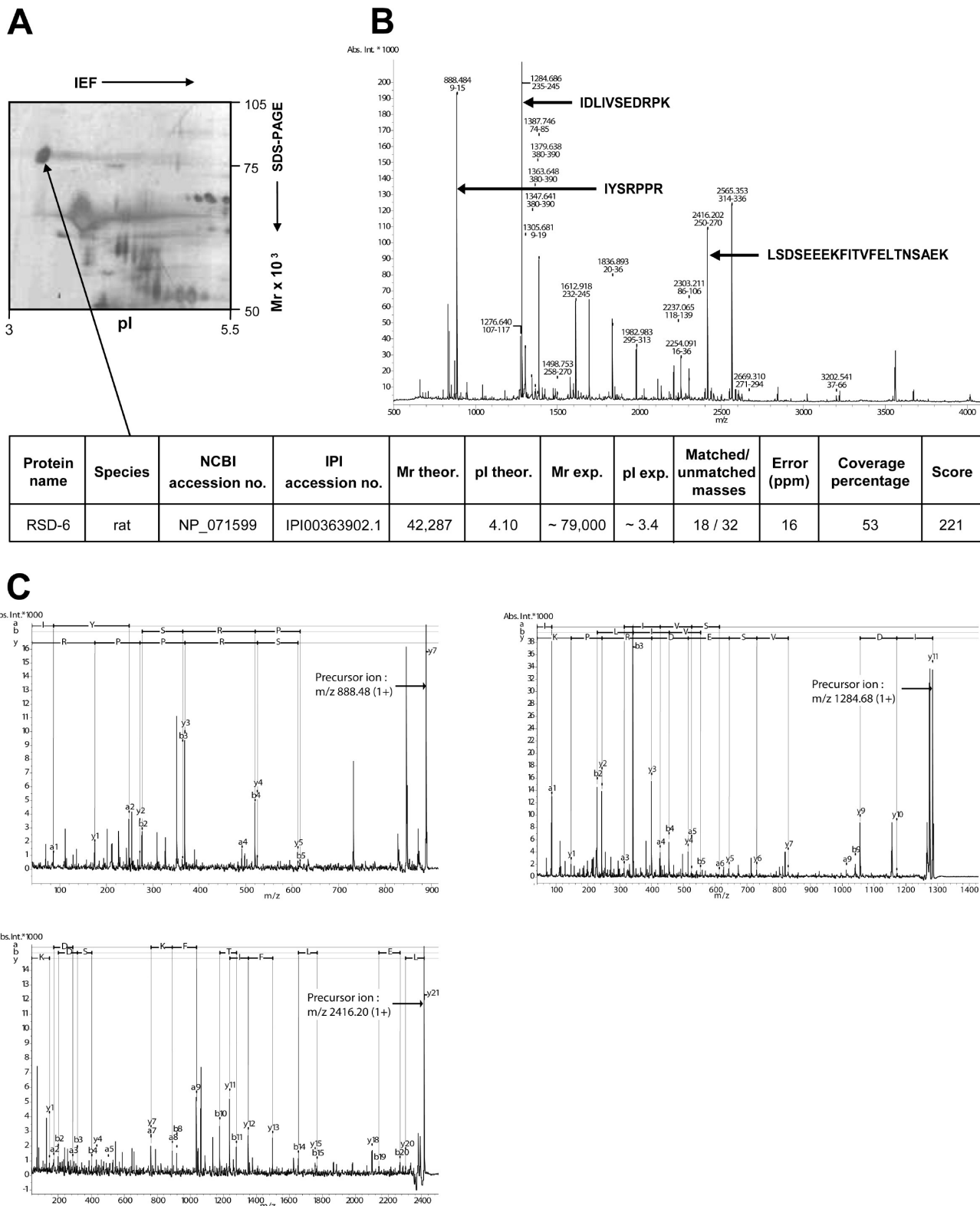


**Figure 1.** Identification by mass spectrometry of CLPH in rat spermatid protein extracts. (A) Cropped image of a silver-stained 2D electrophoresis gel loaded with 150  $\mu$ g of rat spermatid protein, using a nonlinear pH 3–10 18-cm IPG strip for isoelectric focusing and a 12% SDS-polyacrylamide gel for SDS-PAGE. The protein spot identified as the hypothetical rat protein RSD-6 is indicated by an arrow. This figure is an enlargement of the CLPH area (pH 3–5.5) after 2D electrophoretic separation. Protein name, NCBI and IPI accession numbers, theoretical and experimental  $M_r$ , theoretical and experimental pl, matched and unmatched peptides, error, coverage percentage and Mascot protein score are indicated in the table. (B) Mass spectra allowed the identification of rat CLPH by peptide mass fingerprinting and by providing sequence information for the 888.48, 1284.68, and 2416.20 Da peptides, indicated by arrows. (C) MS/MS spectra of the 888.48, 1284.68, and 2416.20 Da peptides.

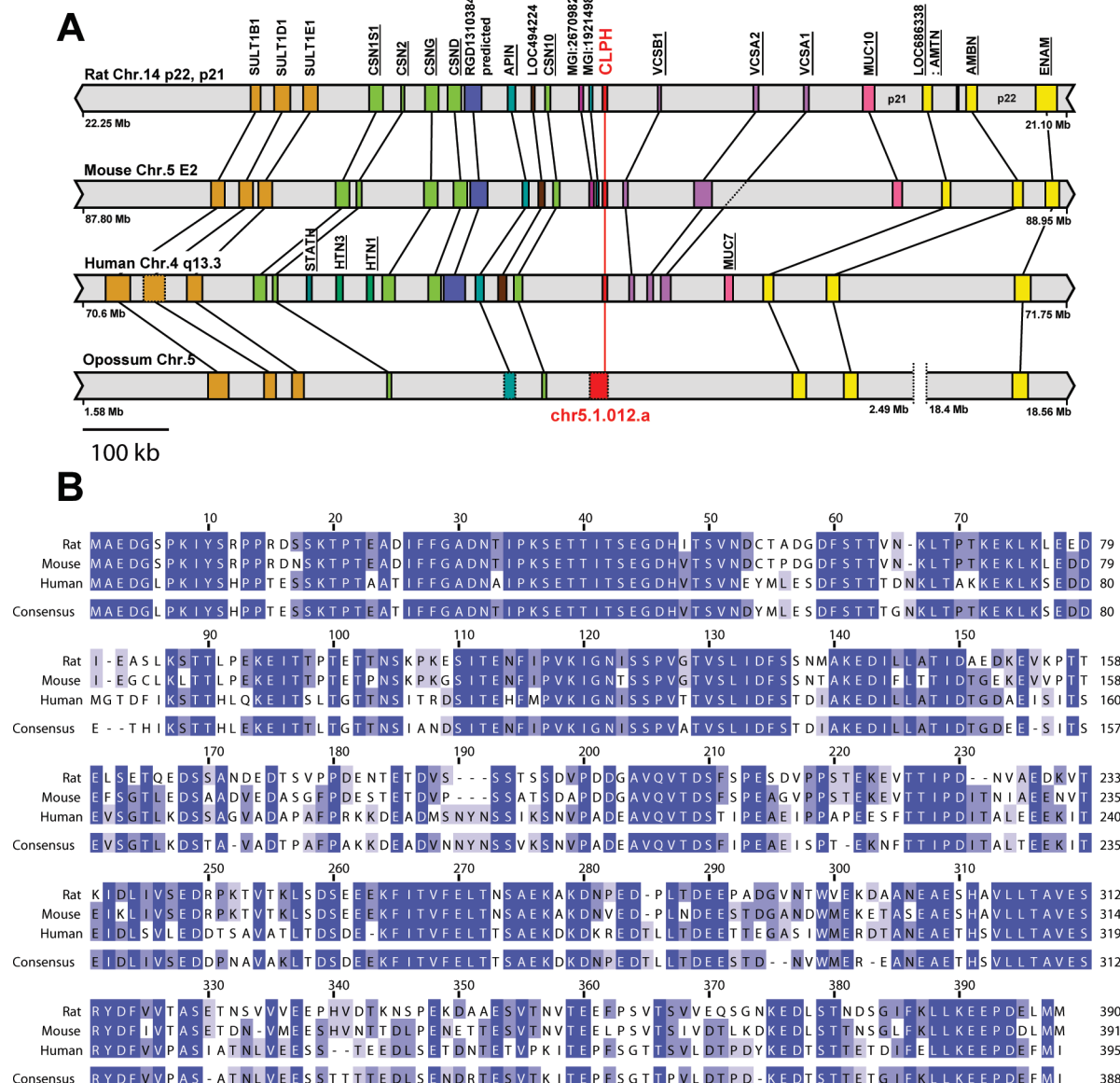


**Figure 2.** Genomic localization and amino acid sequences of predicted rat, mouse, human and opossum CLPH orthologs. (A) The predicted locations of orthologous genes for CLPH (rat: *Rsd-6*; mouse: *4931407G18Rik*; human: *C4orf35*; opossum: *chr5.1.012.a*) are shown by red boxes. The rat genes previously described as SCPP genes are underlined. Continuous-line boxes indicate annotated genes, whereas dashed-line boxes represent predicted genes (Ensembl genome browser). All rat, mouse, human and opossum orthologs at the loci shown are linked by a continuous line. (B) ClustalW multiple alignment of the rat CLPH protein (IPI00363902.1) with its mouse (IPI00226033.2) and human (IPI00328711.5) orthologs, and the consensus sequence resulting from overall multiple alignment of the previously cited 17 eutherian gene products. Dark blue areas with a white font indicate identical preserved amino acids.

scans, with subtraction of the baseline recorded for the buffer solution (i.e., 20 mM sodium phosphate pH 7.2) at 37 °C. The concentration of  $\text{recCLPH}$  protein was 0.965 mg/mL. The cylindrical cells used for far-UV measurements (185–260 nm) had a path length of 0.01 cm. Bovine  $\beta$ -lactoglobulin (1.275 mg/mL) and bovine  $\beta$ -casein (1.169 mg/mL) were used as controls for globular  $\beta$ -proteins and disordered proteins, respectively, and were analyzed under similar conditions.

**Fluorescence Studies.** Fluorescence was measured with a F-4500 spectrofluorimeter (Hitachi, Tokyo, Japan) equipped with a 150 W xenon lamp and a thermostat-controlled bath. Tryptophan emission fluorescence spectra were recorded for the  $\text{recCLPH}$  protein in 20 mM sodium phosphate, pH 7.2, at 37 °C. The excitation wavelength was set at 296 nm and the emission wavelength was tuned from 300 to 400 nm. The width

of both excitation and emission slits was set at 5.0 nm. The fluorescence emission of two tryptophan-containing proteins (i.e., bovine  $\beta$ -lactoglobulin and bovine  $\beta$ -casein), was also measured as control. The background fluorescence of sodium phosphate buffer alone was recorded under similar conditions and subtracted from all spectra.

## Results

**CLPH, a New Protein Identified in Rat Spermatids.** Proteomic analysis of rat spermatids by two-dimensional electrophoresis (2DE) combined with mass spectrometry led to the identification of a peptide with a  $M_r$  of 79 000 and a  $pI$  of 3.4, corresponding to a hypothetical protein annotated by accession number NP\_071599.2 and named RSD-6 for Rat Sperm DNA number 6 (Figure 1A). We named this hypothetical protein

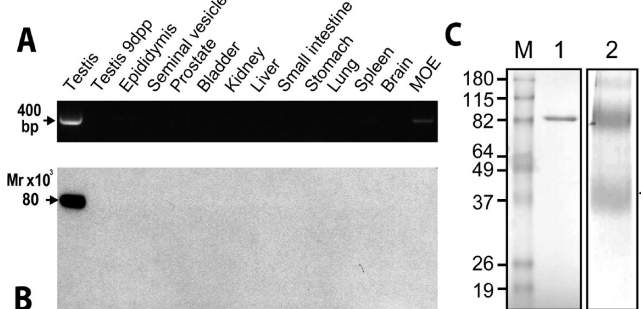


**Figure 3.** (A) RT-PCR analysis of CLPH transcript levels in various rat organs. (B) Western blot analysis of CLPH protein levels in various rat organs. The study was performed with total organ protein extracts (20 µg of protein), and a polyclonal antibody directed against the full-length rat CLPH. *rec*CLPH protein was used as a positive control for the CLPH antibody (data not shown). MOE: Main olfactory epithelium. (C) Chemical modification of *rec*CLPH. 10% SDS-PAGE. M: molecular mass standards; lane 1, unmodified *rec*CLPH (2 µg); lane 2, EDC-modified *rec*CLPH (10 µg). Arrowhead indicates the 44 kDa-migrating *rec*CLPH.

CLPH for *Casein-Like PHosphoprotein*. The experimental  $M_r$  and pI values both differ considerably from the calculated values— $M_w$  (42 287 kDa) and pI (4.1)—for CLPH. The number of matched peptides extracted from the mass spectrum (Figure 1B), covering most of the CLPH protein sequence (18 unique peptides identified, 53% sequence coverage), was sufficient for unambiguous identification by peptide mass fingerprinting with Mascot search engine in MALDI-TOF experiments. In addition, the sequencing of three peptides of 888.48, 1284.68, and 2416.20 by tandem mass spectrometry confirmed the result (Figure 1C).

**Conservation of *Cph* Gene Structure and Sequence During Evolution.** We investigated the conservation of the gene, by aligning the rat *Cph* gene (previously annotated as *Rsd-6* gene, chromosome 14, from 21 616 284 to 21 618 346 on the minus strand; Figure 2A) with the vertebrate genomes available on the UCSC genome browser and Ensembl geneview (Ensembl rat gene ID: ENSRNOG00000001950) Web sites. Orthologous genes were found exclusively in placental mammals, including *Homo sapiens* (annotated as *C4orf35* gene and Testis Development Protein NYD-SP26 in Ensembl database), *Mus musculus* (annotated as *4931407G18Rik* gene and Testis Development Protein NYD-SP26 homologue in Ensembl database), *Bos taurus*, *Canis familiaris*, *Dasypus novemcinctus*, *Echinops tel-fairi*, *Equus caballus*, *Felis cattus*, *Macaca mulatta*, *Microcebus murinus*, *Myotis lucifugus*, *Oryctolagus cuniculus*, *Otolemur garnettii*, *Pan troglodytes*, *Pongo pygmaeus* and *Tupaia belangeri* (all annotated as Testis Development Protein NYD-SP26 homologue in Ensembl database). In addition, the rat and human CLPH proteins were unambiguously mapped by Ensembl Blastview to the 3' end (chromosome 5, from 2 138 157 to 2 139 200) of a gene predicted by N-Scan and called chr5.1.012.a, in the opossum genome (Figure 2A). All these orthologous genes seem to be located in chromosomal regions syntenic to the rat locus (Figure 2A). No orthologous genes were found in nonmammalian vertebrate genomes and no paralogous gene were found in rat, mouse and human genomes by Ensembl Blastview.

**CLPH is Found in the Testis and Is Specifically Produced in Spermatids.** RT-PCR analyses on a large array of rat tissues showed that the CLPH transcript was produced in large

amounts in the testis, whereas a weak signal was observed in the main olfactory epithelium (MOE, Figure 3A).

The protein was detected by Western blotting in total adult testicular extracts (Figure 3B). No signal was detected in any of the other organs tested, including the main olfactory epithelium (Figure 3B) and no signal was detected in total testis extracts when the CLPH antiserum was first incubated with *rec*CLPH protein (data not shown). Of note is that CLPH protein was detected at a  $M_r$  of 80 kDa rather than at its expected molecular weight of 42 kDa, in all experiments based on 1D and 2D SDS-PAGE migration (Figure 1A). Such a discrepancy is often due to glycosylation which retards migration. On another hand, similarly retarded migration profiles have also been reported for very acidic and intrinsically disordered proteins. In these proteins, negatively charged regions do not bind SDS correctly,<sup>23,29</sup> resulting in a slower migration of the protein under denaturing conditions. We thus treated *rec*CLPH, which showed a similar electrophoretic shift onto SDS-PAGE gels (Figure 3C, lane 1), with carbodiimide/ethanolamine in order to neutralize the negatively charged carboxyl groups of acidic residues. A migration profile appropriate to the theoretical molecular weight (i.e., 44 kDa) was partially produced by the treatment (Figure 3C, lane 2), suggesting that the standard electrophoretic character of CLPH may be due to its acidic nature rather than the presence of polysaccharide chains.

In rats, classification of the seminiferous epithelium cycle by Leblond and Clermont<sup>30</sup> defines 14 stages (from I to XIV) in which spermiogenesis, which refers to the morphological transformation of spermatids into spermatozoa, involves 19 differentiation steps (from 1 to 19). *In situ* hybridization experiments on adult rat testis sections clearly showed that the CLPH transcript was present in the seminiferous tubules only in spermatids at steps 4–14 (stages IV–XIV of the seminiferous epithelium classification) (Figure 4A,B,E), with levels of this transcript being highest in spermatids at steps 8–10 (stages VIII–X) (Figure 4B,E). No signal was detected in other germ cells or in testicular somatic cells.

Immunochemical studies revealed that the protein was also present exclusively in the seminiferous tubules (Figure 4C). In these tubules, staining was weak in step 10 spermatids (stage X) (Figure 4C,F), subsequently increasing to reach maximal levels in the cytoplasm of step 18 elongated spermatids (stage VI) (Figure 4C,F). The residual bodies, corresponding to the portions of the cytoplasm of elongated spermatids shed at the time of spermiation, were also stained (Figure 4D), whereas only a weak signal was detected in the cytoplasmic droplets of the spermatozoa released into the tubule lumen (Figure 4D). No staining over background levels was visible in other germ cells or in somatic cells from the seminiferous tubules. Interestingly, in the head segment of the epididymis, the cytoplasmic droplets of spermatozoa retained their immunoreactivity, whereas only residual staining was observed in the tail region (data not shown).

The subcellular localization of CLPH in spermatids was refined, by carrying out transmission electron microscopy analysis on ultrathin sections of adult testes. Immunogold particles were not detected in the middle section of elongated spermatids, but were frequently encountered as grouped structures in the cytoplasm of these cells (Figure 5A). A significant CLPH signal was consistently observed in the mitochondria of step 17 to 18 spermatids. The images obtained strongly suggest that CLPH was associated with the mitochondrial inner membrane in step 18 spermatids (Figure 5B). No

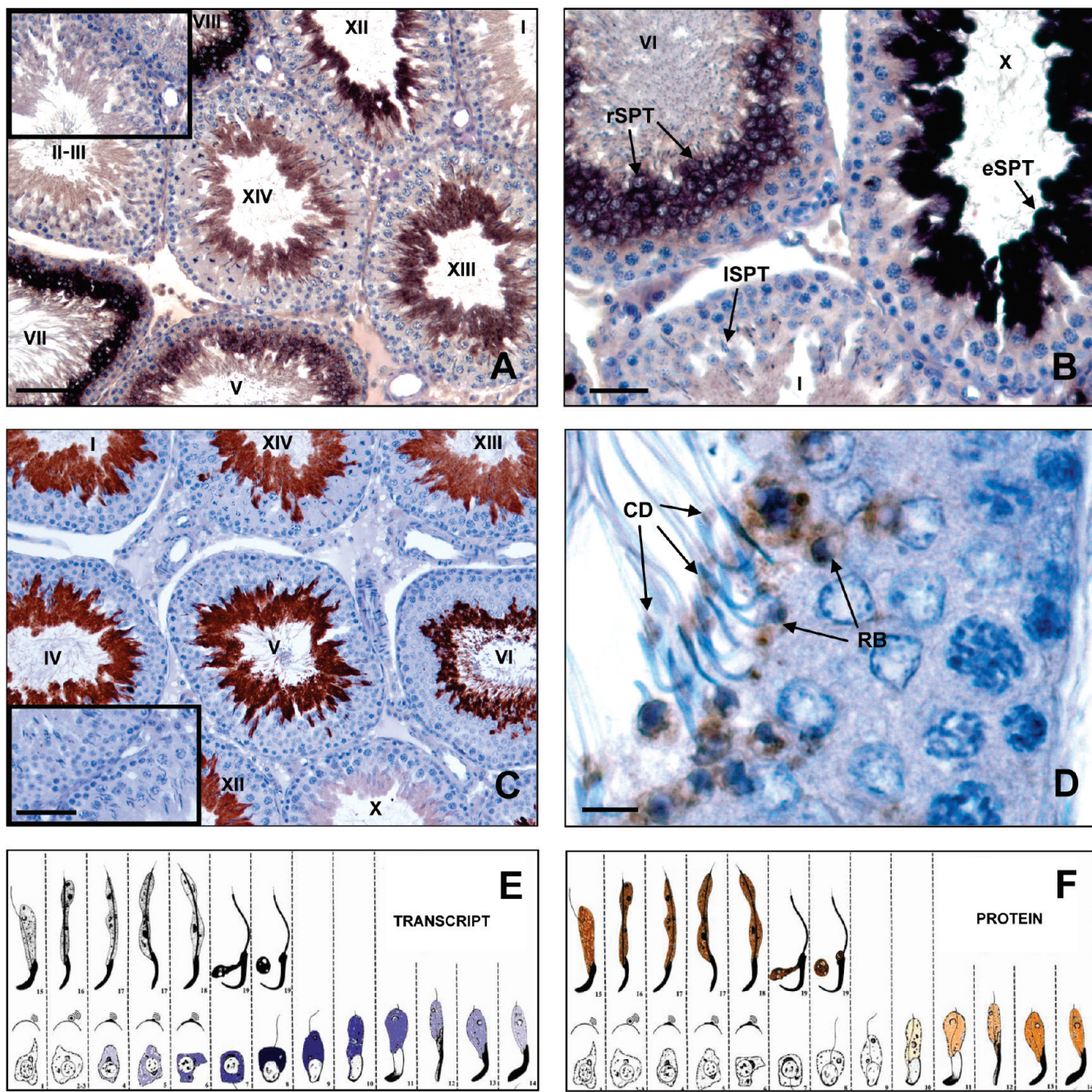


**Figure 4.** *In situ* hybridization and immunolocalization of CLPH in the adult rat testis. In A, B and C, roman numerals indicate seminiferous epithelium stages.<sup>30</sup> *In situ* localization of the CLPH transcript in the adult rat testis. *In situ* hybridization experiments were carried out on serial paraffin sections of rat testis, with antisense (T7 RNA polymerase with *Bam*H-linearized vector) or control sense (T3 RNA polymerase with *Kpn*I-linearized vector; inset in A) dioxygenin-labeled probes. (A) A transverse section of the testis of an adult rat showing very strong labeling in round and elongating spermatids, Scale bar = 100  $\mu$ m. (B) A transverse section of a testis from an adult rat at higher magnification, showing strong labeling of the cytoplasm of round spermatids (rSPT) at stage VI. Very intense and specific labeling was observed in the cytoplasm of elongating spermatids (eSPT) at stage X, whereas no signal was observed in step-15 long spermatids (ISPT) or spermatids at later stages. Scale bar = 50  $\mu$ m. Immunolocalization of CLPH protein in the adult rat testis. Organs were fixed by immersion in Bouin's fixative solution. CLPH was detected with a specific rabbit polyclonal antiserum raised against the rat recombinant protein, as described in Experimental Procedures. Experiments were carried out on serial rat testis sections with a preimmune serum as a negative control (inset in C). (C) Transverse section of a testis from an adult rat showing increasing, strong CLPH immunoreactivity in elongating spermatids from stage X to stage VI. Scale bar = 100  $\mu$ m. (D) Transverse section of a testis from an adult rat at higher magnification showing strong CLPH immunoreactivity in the residual bodies (RB) and in the cytoplasmic droplets (CD) of spermatozoa. Bar = 10  $\mu$ m. Lower panels show summaries of CLPH transcript (E; blue) and protein (F; brown) *In situ* localization superimposed on the map of spermatogenesis from Leblond and Clermont,<sup>30</sup>as modified by Dym and Clermont.<sup>54</sup>

particles were observed when the primary antibody was omitted (data not shown).

**Computer Analysis of CLPH Protein Sequences.** The CLPH protein, like the structure of the gene encoding it, appears to

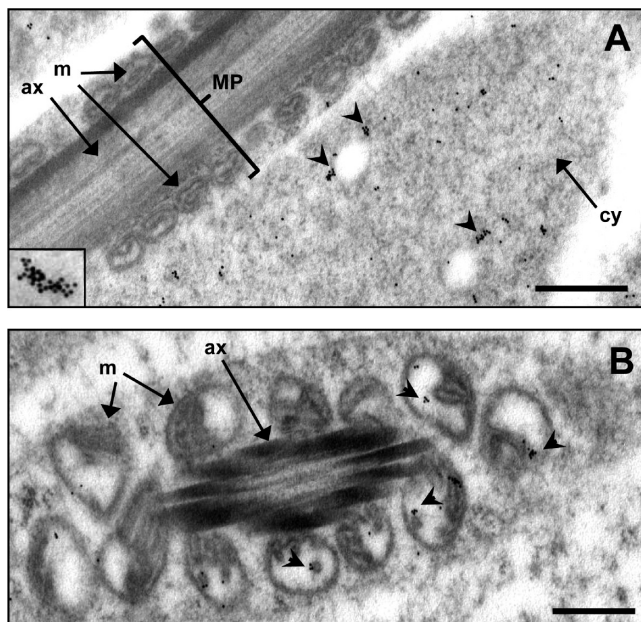


**Figure 5.** Subcellular localization of CLPH protein in adult rat testis by transmission electron microscopy. Immunogold particles are indicated by arrowheads. (A) Gold particles are frequently associated into grouped structures (inset) in the cytoplasm of elongating and elongated spermatids, whereas no signal is detected in the middle part of these cells. Scale bar = 500 nm. (B) Transverse section of a step 18 spermatid displaying mitochondrial staining. Gold particles are mostly associated with the mitochondrial inner membrane. MP, middle part; m, mitochondrion; ax, axoneme, cy, cytoplasm. Scale bar = 500 nm.

be highly conserved within placental species. Indeed, the rat amino acid sequence displayed 81% and 60% identity to the mouse and human proteins, respectively (Figure 2B). ScanProsite analyses of the rat peptide sequence revealed the presence of a single N-myristylation site (PS00008), three N-glycosylation sites (PS00001), and a canonical EF-hand type calcium-binding domain (PS00018). This last motif (DSEEEK-FITVFE, aa 252–263 in the rat) is conserved in 12 species, not including human, orangutan, chimpanzee and hedgehog, due to point mutations resulting in single amino acid changes.

Finally, scansite analysis of the rat peptide showed the presence of two Casein kinase 2 phosphorylation sites, the most relevant (score: 0.3898) being located on T<sub>280</sub>.

**CLPH Is Phosphorylated *In Vivo*.** We investigated whether CLPH protein was phosphorylated *in vivo*, by immunoprecipitating the native protein from rat spermatid protein extracts and analyzing it further by nano-LC-MS/MS. The CID MS<sup>2</sup> spectra of 623 compounds were processed with the Mascot search engine and led to the identification of 27 unique peptides, covering 62% of CLPH peptidic sequence (score: 1271). Among the matching peptides, a 2747.8774 Da threonine-phosphorylated peptide (retention time: 38.5 min) was identified, together with its unmodified 2668.0354 Da analogue (retention time: 37.3 min) (Table 1). Similar results were obtained using the Phenyx search engine (data not shown). The phosphorylation was attributed by low energy CID analysis of both modified and unmodified peptide to the threonine residue located in position 280, the one previously proposed as a putative CK2 phosphorylation site by the Scansite analysis of the rat protein (Figure 6). Of note is that, in many cases, CID MS<sup>2</sup> spectra of the phosphopeptide displayed two different

mass values for the same fragment ion when compared to the unmodified peptide, with either an 80 Da increment or an 18 Da decrement (Figure 6). This loss of 98 Da can be attributed to the partial  $\beta$ -elimination of phosphoric acid that occurs during low energy CID fragmentation of phosphothreonyl peptides.<sup>31</sup>

***rec*CLPH Is Phosphorylated *In Vitro* by Casein Kinase 2.** We determined whether CLPH was indeed a substrate of casein kinase 2 (CK2), by carrying out phosphorylation experiments with the recombinant form of rat CLPH we had prepared. Autoradiography showed that *rec*CLPH and caseins were phosphorylated by CK2, with higher phosphorylation efficiency for caseins (Figure 7). In both cases, the reaction was strongly inhibited in the presence of heparin (Figure 7, lanes 6 and 9). The residual signal detected by autoradiography for CLPH in the absence of enzyme (Figure 7, lane 4) or with heparin (Figure 7, lane 6) may be due to nonspecific polar interactions between  $\gamma^{32}\text{P}$ -ATP and the CLPH protein. As expected, bovine serum albumin (BSA) was not phosphorylated by CK2 (Figure 7, lane 3) and CK2 was not detected by autoradiography (Figure 7, lane 1) or in Coomassie blue stained gels (data not shown). Additionally, the analysis of the trypsin-digested CK2-phosphorylated recombinant CLPH by nano-LC-MS/MS indicates that the threonine located in position 280 was mainly under a phosphorylated form, whereas no such modification was observed in the untreated *rec*CLPH (data not shown).

**CLPH Is a Calcium-Binding Protein.** On the basis of our motif predictions, which suggested that CLPH harbors a putative conserved calcium binding site, we investigated the calcium binding properties of this protein. The incubation of membrane-blotted *rec*CLPH with  $^{45}\text{Ca}^{2+}$  resulted in a strong signal on exposed autoradiography film (Figure 8A, lane 3), whereas BSA processed under similar conditions gave only a slight residual signal (Figure 8A, lane 1). As expected, bovine caseins also gave a strong signal (Figure 8A, lane 2), in an extent similar to that seen for *rec*CLPH (Figure 8B, lanes 2 and 3).

**CLPH Is an Intrinsically Disordered Protein.** The CLPH protein harbors certain features typical of intrinsically disordered proteins, such as a large proportion of charged amino acids, mostly acidic (23.3% of D and E) and a small proportion of aliphatic residues. Indeed, the calculated mean net charge ( $\langle R \rangle_{\text{CLPH}} = 0.146$ ) and mean hydrophobicity ( $\langle H \rangle_{\text{CLPH}} = 0.421$ ) classify CLPH as a predicted natively unfolded protein, according to Uversky's relationship ( $\langle R \rangle = 2.785 \langle H \rangle - 1.151$ ).<sup>32</sup> An analysis of the amino acid sequence with the FoldIndex program also highlighted the putative existence of large disordered domains within the protein (Figure 9A).

As sensitivity to protease digestion is a good indicator of the level of compaction of a protein,<sup>33</sup> we compared the digestion kinetics of *rec*CLPH with those of BSA, a known globular protein, in the presence of increasing amounts of porcine trypsin (Figure 9B). This experiment clearly showed that *rec*CLPH was trypsin-hypersensitive, as this protein was completely degraded by incubation with trypsin at a ratio of 1/800 (Figure 9B, lane 5), whereas BSA remained merely intact under similar conditions (Figure 9B, lane 11).

We also evaluated intrinsic disorder by carrying out a circular dichroism analysis of *rec*CLPH protein (Figure 9C). A strong negative peak was detected at about 197 nm on the far-UV spectrum, whereas a small inflection was seen in the 220–230 nm region of the spectrum. This spectrum shape was close to that observed for  $\beta$ -casein and is typical to intrinsically disordered proteins, as defined by Dunker.<sup>34</sup> Finally, we

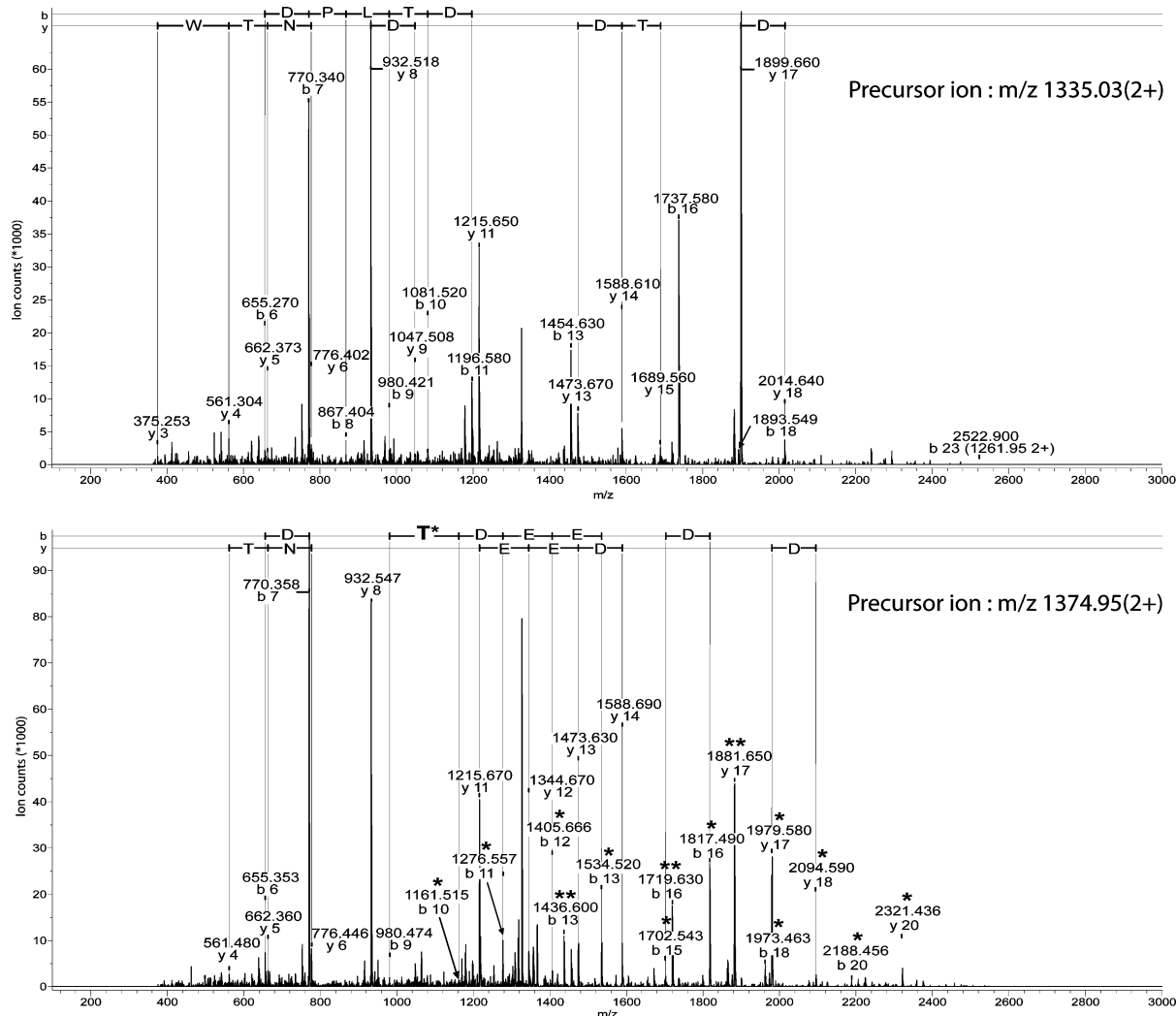


**Figure 6.** CLPH is a phosphoprotein. CID spectra of the unmodified tryptic peptide eluting at 37.3 min, <sup>27</sup>AKDNPEDPLTDEEP-ADGVNTWVEK<sub>294</sub> (upper panel) and of its T<sub>280</sub>-phosphorylated analogue eluting at 38.5 min (lower panel). \*, phosphothreonyl fragment ions; \*\*, loss of H<sub>3</sub>PO<sub>4</sub> (-98 Da).

**Table 1.** Peptides Detected by LC-MS

ion detected	MH <sub>expected</sub>	MH <sub>calculated</sub>	Δ[Da]	miss.	ion score	peptide
1335.0250(2+)	2668.0354	2668.2140	-0.1786	1	41	K.AKDNPEDPLTDEEPADGVNTWVEK.D
1374.9460(2+)	2747.8774	2748.1803	-0.3029	1	49	K.AKDNPEDPLT*DEEPADGVNTWVEK.D (+ Phospho T)

measured the emission of fluorescence by tryptophan in the rat recombinant protein at an excitation wavelength of 296 nm. recCLPH exhibited a maximal fluorescence at the 350 nm-wavelength (Figure 9D), a value similar to that obtained with free tryptophan in solution.<sup>35</sup> In comparison, the bovine  $\beta$ -lactoglobulin showed a clear blue shift of its maximum fluorescence by as much as 20 nm (Figure 9D).

## Discussion

Germ cell differential protein expression profiling during spermatogenesis was recently assessed by our group thanks to the 2D-DIGE technology. With this technique, we identified a large set of proteins with relative abundances differing significantly between spermatogonia, spermatocytes and spermatids. We have demonstrated the specific presence of a previously unknown protein that we called CLPH, in the extracts prepared from purified rat spermatids. We describe

here further investigation of CLPH protein and mRNA production within the testis, together with insights on the characterization of the protein.

The rat *Clph* gene, which is located on chromosome 14.p21, was mapped in the genomes of 16 other mammalian species. The identified orthologs of the *Clph* gene are all located on a chromosomal region syntenic to the cluster of milk and salivary secretory calcium-binding phosphoprotein (SCPP) genes (chromosome 4q13.3 for humans and chromosome 5E2 for mice). These mammal-specific genes, encoding many secreted proteins such as caseins are involved in the mineralization of enamel, milk and saliva,<sup>36</sup> have highly conserved positions and orientations in mammalian genomes and are thought to have arisen from a single ancestral gene.<sup>37</sup> We therefore hypothesize that *Clph* may also be derived from this ancestral gene. Indeed, this gene and the protein it encodes share many of the unusual characteristics of SCPP genes and proteins: (1) *Clph* is specific

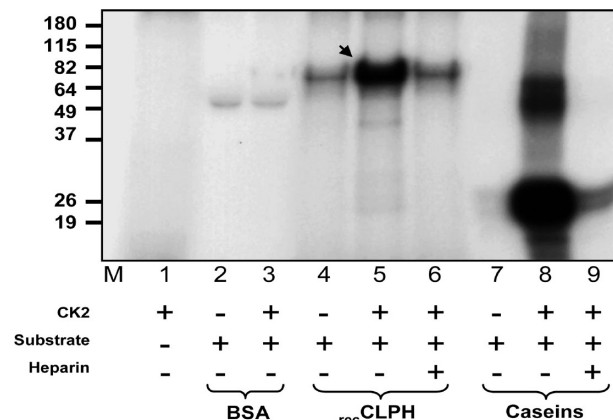


**Figure 7.** CLPH is phosphorylated *in vitro* by casein kinase 2. *In vitro* phosphorylation of full-length *rec*CLPH by rat casein kinase 2. Extracts were resolved by SDS-PAGE and *in vitro* phosphorylated proteins were detected by autoradiography. Bovine serum albumine (lanes 2, 3), *rec*CLPH (lanes 4, 5, 6) and a mixture of bovine  $\alpha$ ,  $\beta$  and  $\kappa$  caseins (lanes 7, 8, 9) were incubated in the absence (-) or presence (+) of casein kinase 2. CK2 inhibition by heparin was tested for CLPH (lane 6) and caseins (lane 9). As a control, CK2 was incubated alone in reaction buffer to evaluate the autophosphorylation signal (lane 1). The phosphorylated form of CLPH is indicated by an arrowhead.

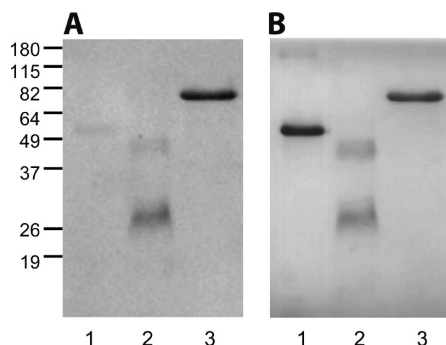


**Figure 8.** CLPH is a calcium-binding protein. Protein samples (6  $\mu$ g) were blotted onto a PVDF membrane after SDS-PAGE. The  $^{45}\text{Ca}^{2+}$ -binding capacity of each sample was evaluated by autoradiography. (A) Autoradiograph; (B) Ponceau-stained PVDF membrane before  $^{45}\text{Ca}^{2+}$  incubation. Lane 1, BSA; lane 2, bovine caseins; lane 3, *rec*CLPH.

to mammals and expressed in a tissue-specific manner; (2) in addition to its conserved chromosomal synteny with SCPP genes, *Clph* shares the same codon usage (i.e., enrichment in X-X-(A/T) codons<sup>38</sup>); (3) in rats, mice and humans, the CLPH protein contains a high proportion of acidic and basic amino acids and smaller proportions of aliphatic residues;<sup>36</sup> (4) CLPH is a phosphoprotein; (5) CLPH strongly binds calcium; (6) CLPH is intrinsically disordered, as previously reported for known SCPPs, such as caseins<sup>39</sup> and salivary proline-rich proteins.<sup>40</sup> Nevertheless, CLPH has no N-terminal secretion tag, but it is likely that this tag, should it had existed, was eliminated during evolution by genetic reshuffles, due to the lack of associated strong functional constraints.

We report here that the production of CLPH protein is restricted to the testis in rats and mice. RT-PCR showed very low levels of transcript in the main olfactory epithelium of rats, consistent with the results of the transcriptomic profiling of mouse tissues available on Symatlas database (<http://symatlas.gnf.org>). Reliably, the mouse gene (annotated as 4931407-

G18Rik), was previously proposed among 99 others as a cilia-related gene, that is, genes which share a high-abundance expression profile in ciliated cells-containing organs, such as the testis and the olfactory epithelium.<sup>41</sup> This may be an important issue, given the well-established biological correspondence between olfactory signaling mechanisms and sperm maturation and motility.<sup>42</sup> However, we detected no CLPH by Western blotting or immunohistochemical experiments neither on the rat main olfactory epithelium nor on the sperm surface, indicating that the very little, if any, of this transcript is translated.

*In situ* hybridization experiments showed that the CLPH transcript was specifically produced in round postmeiotic spermatids. These results are consistent with those obtained in a recent transcriptomic profiling of spermatogenesis in the mouse.<sup>43</sup> Immunohistochemistry experiments clearly showed CLPH to be produced essentially in elongating and elongated spermatids, whereas it was principally detected in protein extracts from round spermatids in a previous 2D-DIGE analysis of rat spermatogenesis.<sup>13</sup> This divergence may be accounted for by the contamination of isolated round spermatid preparations with elongated spermatids and residual bodies.<sup>14</sup> Alternatively, immunohistochemical methods are not particularly sensitive, whereas the proteomic experiment was performed with extracts of an enriched preparation of early spermatids (i.e., steps 1–8), that is, with very concentrated spermatid proteins. In any case, even if CLPH is produced in small amounts in the pre-elongating spermatids, this does not affect its general expression profile. The delay observed here between the end of gene transcription in elongating spermatids and the peak of protein production in late elongated spermatids and residual bodies probably reflects the large number of spermatid- and sperm-specific transcripts for which translation is enhanced during spermatid elongation, after storage and repression in the chromatoid bodies of the round spermatids (for review, see ref 44). Taken together, our data suggest that CLPH operates through very specific processes restricted to the postmeiotic germ cell line.

Electron microscopy experiments showed that CLPH was present mostly in the cytoplasm of late spermatids, but also frequently associated with the mitochondrial inner membrane. Interestingly, CLPH seemed to aggregate into coherent structures in the cytoplasm of the elongated spermatids. This suggests that the protein may form multimeric complexes, the composition of which remains to be elucidated. This hypothesis is supported by exclusion chromatography and native electrophoresis experiments showing that *rec*CLPH resolved into several distinct entities (data not shown).

Considering that phosphorylation is an important post-translational modification (PTM) enhancing the function of many proteins, including SCPPs,<sup>45,46</sup> we carried out nano-LC-MS/MS analysis to investigate the occurrence of phosphorylation events in native CLPH. The peptide  $_{271}\text{AKDNPDPEPLT-DEEPADGVNTWVEK}_{294}$  was found together with an additional chromatographically latter eluting peak, corresponding to an 80 Da modified analogue. MS<sup>2</sup> analysis of both peptides by low energy CID fragmentation showed the modification to be borne by the Thr<sub>280</sub> and was identified as a phosphorylation by Mascot and Phenyl search engines. This result is consistent with our *in silico* analysis of rat CLPH sequence that described this residue as a highly probable CK2 phosphorylation site. Nevertheless, the existence of isobaric 80 Da PTMs such as threonine O-sulfonation has been previously reported<sup>31</sup> and

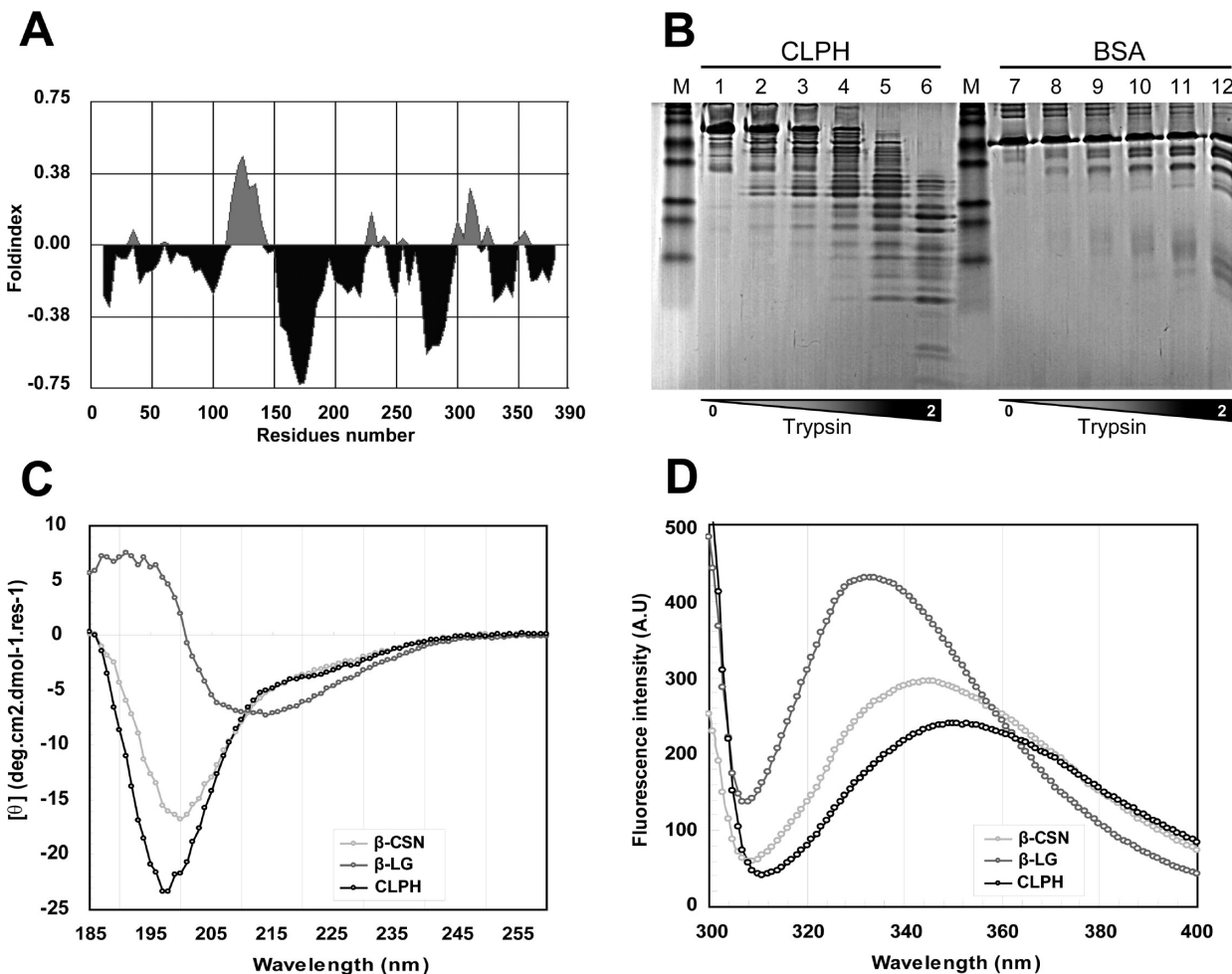


**Figure 9.** CLPH is an intrinsically disordered protein. (A) A FoldIndex plot was obtained with a window of 20 residues and a 5-residue step; dark areas below zero indicate unfolded regions, whereas clear areas above zero correspond to predicted folded regions. (B) Tryptic digests of <sub>rec</sub>CLPH protein and BSA. Ten micrograms of <sub>rec</sub>CLPH (lane 1–6) or BSA (7–12) was incubated at a final concentration of 0.8 mg/mL with 0, 0.0625, 0.125, 0.25, 0.5, 1, and 2 µg/mL of porcine trypsin for 30 min at 37 °C. Digests were analyzed by SDS-PAGE in a 15% polyacrylamide gel. (C) Circular dichroism spectra of <sub>rec</sub>CLPH, bovine β-lactoglobulin and bovine β-casein in 20 mM sodium phosphate, pH 7.2, at far-UV wavelengths. Molar ellipticity [θ]MRW was calculated from the measured ellipticity (θ, in millidegrees), according to the following formula: [θ]MRW = θ × 100/(nlc), where n is the number of amino acid residues, c is the total concentration (mM), and l is the cell path length (cm). (D) Measurement of the tryptophan fluorescence emitted by <sub>rec</sub>CLPH, bovine β-lactoglobulin and bovine β-casein.

could lead to a misinterpretation of MS<sup>2</sup> data. However, the different CID behavior of sulfonated and phosphorylated peptides has been extensively studied and proved to be a valuable element to distinguish between these two PTMs.<sup>47</sup> Actually, the phosphorylated serine and threonine are known to undergo partial β-elimination of H<sub>3</sub>PO<sub>4</sub> (98 Da) during CID analyses. The resulting fragment ions in MS<sup>2</sup> spectra thus exhibit a +80 Da or a -18 Da mass shift, when compared to the corresponding unmodified peptides fragments. This phenomenon is not observed in the case of sulfonated peptides under similar analytical conditions. Consistently, we were able to find at least three H<sub>3</sub>PO<sub>4</sub>-depleted fragment ions together with their modified analogues, thus, clearly indicating that this PTM is a phosphorylation rather than a sulfonation.

In the present study, *in vitro* casein kinase 2 phosphorylation assays with <sub>rec</sub>CLPH showed this protein to be strongly phosphorylated by CK2, especially on T<sub>280</sub>. Our experiments confirmed that this site is fully available for CK2 phosphorylation, thus, suggesting the importance of this PTM in the enhancement of CLPH function during spermiogenesis. In this context,

the fact that CLPH may well be a new testicular target of CK2 is of considerable potential interest, given the major impact of CK2 on the progress of mammalian spermatogenesis, especially in the shaping of sperm head and tail.<sup>48,49</sup> Considering the absence to date of validated substrate for CK2 in haploid germ cells, the characterization of CLPH function may therefore provide considerable insight into the role of CK2 in spermatogenesis.

We also showed that CLPH strongly binds calcium. However, the way it does remains unclear. In most of EF-hand-containing proteins, these motifs tend to be associated in pairs,<sup>50</sup> but this is not the case in CLPH. The calcium-binding capacity of CLPH may also be linked to its acidic status. Indeed, many calcium-binding proteins, such as calsequestrin<sup>51</sup> and FSCB,<sup>27</sup> lack EF-hand motifs but nonetheless bind calcium through negatively charged regions. The presence of at least one long acidic region in rat CLPH that could potentially bind calcium (position 148–230; 29.5% of D + E) supports this hypothesis. Although it has been well-established that the motility and fertilizing ability of ejaculated spermatozoa strongly rely on intracellular calcium concentration,<sup>52</sup> the precise role of calcium in haploid

germ cells remains unclear. In the rat elongated spermatids, calcium deposits have been described along the nuclear membrane and within nuclear matrix, but also in the cytoplasm.<sup>53</sup> Given the strong genetic, biochemical and structural similarities between CLPH and other SCPPs, which are known to act as calcium carriers, the possibility that CLPH is involved in the storage and transport of intracellular calcium in haploid germ cells needs further investigation.

Finally, we demonstrated by CD analysis, fluorescence studies and analytical protease digestion that the CLPH protein has a coil-like structure consisting mostly of disordered regions that do not fold independently into stable secondary structures under physiological conditions. The kinetics of CLPH digestion by trypsin demonstrated a considerable flexibility in the structure of the protein. Indeed, it has been shown that the cleavage sites present in the disordered regions of a protein are more flexible and adaptable to the active site of proteases and, thus, more susceptible to protease digestion.<sup>33</sup> Moreover, the strong negative peak detected at about 197 nm on the far-UV spectrum and the inflection seen in the 220 nm region of the spectrum indicated that only a small part of the protein was organized into secondary structures. More specifically, fluorescence studies showed that the emission range of the single tryptophan (W<sub>291</sub>) present in CLPH was typical of a solvated residue, suggesting that this residue is embedded in an unfolded region that could potentially be accessible for regulators and/or interacting proteins. This hypothesis is strengthened by the presence of a phosphorylated threonine (T<sub>280</sub>) in the very close vicinity of the W<sub>291</sub>. Thus, the possibility that phosphorylation and/or calcium binding could be folding up-promoting events that may contribute to the enhancement of CLPH function merits focused attention.

## Conclusion

We report here the identification and characterization of a new disordered testicular protein whose strong tissue and cell specificity, dual subcellular localization, susceptibility to casein kinase 2 phosphorylation and calcium-binding ability are cumulative indices of a key role in the biology of spermatids. We thus propose to designate this protein as CLPH, for Casein-Like PHosphoprotein, a term that encompasses several of its distinctive properties. We are currently developing appropriate knockout mouse models in our laboratory for investigation of the precise role of CLPH in mammalian spermiogenesis.

**Abbreviations:** CK2, casein kinase 2; GAPDH, glyceraldehyde-3-phosphate dehydrogenase; MOE, main olfactory epithelium; CLPH, casein-like phosphoprotein; <sup>rec</sup>CLPH, recombinant CLPH; SCPP, secretory calcium-binding phosphoprotein.

**Acknowledgment.** This work was supported by the Proteomics Core Facility at OUEST-genopole and was funded by INSERM and *Conseil Régional de Bretagne* grants. We thank B. Delaleu for valuable technical assistance with electron microscopy, Y. Choiset for advice concerning the design of circular dichroism experiments, F. Aubry and C. Garnier for stimulating discussions. P. Calvel holds a fellowship from *Institut National de la Santé et de la Recherche Médicale* and *Région Bretagne*. The nucleotide sequence for the rat protein corresponds to the GenBank Accession Number: NC\_005113.2, region: complement (21616-284...21618346). The CLPH peptidic sequences reported in this paper correspond to the following NCBI Protein Database accession numbers: Rat protein (RSD-6): NP\_071599.2; Mouse protein (testis development protein NYD-

SP26): NP\_081907; Human protein (testis development protein NYD-SP26): AAK57455.

## References

- Jégou, B. The Sertoli cell. *Baillière's Clin. Endocrinol. Metab.* **1992**, *6* (2), 273–311.
- Jégou, B. The Sertoli-germ cell communication network in mammals. *Int. Rev. Cytol.* **1993**, *147*, 25–96.
- Gnessi, L.; Fabbri, A.; Spera, G. Gonadal peptides as mediators of development and functional control of the testis: an integrated system with hormones and local environment. *Endocr. Rev.* **1997**, *18* (4), 541–609.
- Sharpe, R. M. Regulation of spermatogenesis. In *The Physiology of Reproduction*, 2nd ed.; Knobil, E.; Neill, J. D., Eds.; Raven Press: New York, 1994; pp 1363–1436.
- Jégou, B.; Pineau, C.; Dupax, A. Paracrine control of testis function. In *Male Reproductive Function, Endocrine Update Series*; Wang, C., Ed.; Kluwer Academic: Berlin, 1999; pp 41–64.
- Zhao, G. Q.; Garbers, D. L. Male germ cell specification and differentiation. *Dev. Cell* **2002**, *2* (5), 537–47.
- de Rooij, D. G.; de Boer, P. Specific arrests of spermatogenesis in genetically modified and mutant mice. *Cytogenet. Genome Res.* **2003**, *103* (3–4), 267–276.
- Matzuk, M. M.; Lamb, D. J. Genetic dissection of mammalian fertility pathways. *Nat. Cell Biol.* **2002**, *4* (Suppl.), s41–49.
- Rolland, A. D.; Jégou, B.; Pineau, C. Testicular Development and Spermatogenesis: Harvesting the Postgenomics Bounty. In *Molecular Mechanisms in Spermatogenesis*; Cheng, C. Y., Ed.; Landes Bioscience: Austin, TX, 2008.
- Huang, S. Y.; Lin, J. H.; Chen, Y. H.; Chuang, C. K.; Lin, E. C.; Huang, M. C.; Sunny Sun, H. F.; Lee, W. C. A reference map and identification of porcine testis proteins using 2-DE and MS. *Proteomics* **2005**, *5* (16), 4205–4212.
- Essader, A. S.; Cargile, B. J.; Bundy, J. L.; Stephenson, J. L., Jr. A comparison of immobilized pH gradient isoelectric focusing and strong-cation-exchange chromatography as a first dimension in shotgun proteomics. *Proteomics* **2005**, *5* (1), 24–34.
- Com, E.; Evrard, B.; Roepstorff, P.; Aubry, F.; Pineau, C. New insights into the rat spermatogonial proteome: identification of 156 additional proteins. *Mol. Cell. Proteomics* **2003**, *2* (4), 248–261.
- Rolland, A. D.; Evrard, B.; Guittot, N.; Lavigne, R.; Calvel, P.; Couvet, M.; Jégou, B.; Pineau, C. Two-dimensional fluorescence difference gel electrophoresis analysis of spermatogenesis in the rat. *J. Proteome Res.* **2007**, *6* (2), 683–697.
- Pineau, C.; Syed, V.; Bardin, C. W.; Jegou, B.; Cheng, C. Y. Germ cell-conditioned medium contains multiple factors that modulate the secretion of testins, clusterin, and transferrin by Sertoli cells. *J. Androl.* **1993**, *14* (2), 87–98.
- Karolchik, D.; Baertsch, R.; Diekhans, M.; Furey, T. S.; Hinrichs, A.; Lu, Y. T.; Roskin, K. M.; Schwartz, M.; Sugnet, C. W.; Thomas, D. J.; Weber, R. J.; Haussler, D.; Kent, W. J. The UCSC Genome Browser Database. *Nucleic Acids Res.* **2003**, *31* (1), 51–54.
- Stalker, J.; Gibbons, B.; Meidl, P.; Smith, J.; Spooner, W.; Hotz, H. R.; Cox, A. V. The Ensembl Web site: mechanics of a genome browser. *Genome Res.* **2004**, *14* (5), 951–955.
- Hulo, N.; Bairoch, A.; Bulliard, V.; Cerutti, L.; De Castro, E.; Langendijk-Genevaux, P. S.; Pagni, M.; Sigrist, C. J. The PROSITE database. *Nucleic Acids Res.* **2006**, *34* (Database issue), D227–230.
- Finn, R. D.; Mistry, J.; Schuster-Bockler, B.; Griffiths-Jones, S.; Hollich, V.; Lassmann, T.; Moxon, S.; Marshall, M.; Khanna, A.; Durbin, R.; Eddy, S. R.; Sonnhammer, E. L.; Bateman, A. Pfam: clans, web tools and services. *Nucleic Acids Res.* **2006**, *34* (Database issue), D247–251.
- Obenauer, J. C.; Cantley, L. C.; Yaffe, M. B. Scansite 2.0: Proteome-wide prediction of cell signaling interactions using short sequence motifs. *Nucleic Acids Res.* **2003**, *31* (13), 3635–3641.
- Larkin, M. A.; Blackshields, G.; Brown, N. P.; Chenna, R.; McGettigan, P. A.; McWilliam, H.; Valentini, F.; Wallace, I. M.; Wilim, A.; Lopez, R.; Thompson, J. D.; Gibson, T. J.; Higgins, D. G. Clustal W and Clustal X version 2.0. *Bioinformatics* **2007**, *23* (21), 2947–2948.
- Prilusky, J.; Felder, C. E.; Zeev-Ben-Mordehai, T.; Rydberg, E. H.; Man, O.; Beckmann, J. S.; Silman, I.; Sussman, J. L. FoldIndex: a simple tool to predict whether a given protein sequence is intrinsically unfolded. *Bioinformatics* **2005**, *21* (16), 3435–3438.
- Menuet, A.; Anglade, I.; Flouriot, G.; Pakdel, F.; Kah, O. Tissue-specific expression of two structurally different estrogen receptor alpha isoforms along the female reproductive axis of an oviparous species, the rainbow trout. *Biol. Reprod.* **2001**, *65* (5), 1548–1557.

- (23) Alves, V. S.; Pimenta, D. C.; Sattlegger, E.; Castilho, B. A. Biophysical characterization of Gir2, a highly acidic protein of *Saccharomyces cerevisiae* with anomalous electrophoretic behavior. *Biochem. Biophys. Res. Commun.* **2004**, *314* (1), 229–234.
- (24) Com, E.; Rolland, A. D.; Guerrois, M.; Aubry, F.; Jegou, B.; Vallet-Erdmann, V.; Pineau, C. Identification, molecular cloning, and cellular distribution of the rat homolog of minichromosome maintenance protein 7 (MCM7) in the rat testis. *Mol. Reprod. Dev.* **2006**, *73* (7), 866–877.
- (25) Castella, S.; Benedetti, H.; de Llorens, R.; Dacheux, J. L.; Dacheux, F. Train A, an RNase A-like protein without RNase activity, is secreted and reabsorbed by the same epididymal cells under testicular control. *Biol. Reprod.* **2004**, *71* (5), 1677–1687.
- (26) Gharib, M.; Marcantonio, M.; Lehmann, S. G.; Courcelles, M.; Meloche, S.; Verreault, A.; Thibault, P. Artifactual sulfation of silver-stained proteins: Implications for the assignment of phosphorylation and sulfation sites. *Mol. Cell. Proteomics* **2008**, *20*, 20.
- (27) Li, Y. F.; He, W.; Jha, K. N.; Klotz, K.; Kim, Y. H.; Mandal, A.; Pulido, S.; Digilio, L.; Flickinger, C. J.; Herr, J. C. FSCB, a novel protein kinase A-phosphorylated calcium-binding protein, is a CAYPR-binding partner involved in late steps of fibrous sheath biogenesis. *J. Biol. Chem.* **2007**, *282* (47), 34104–34119.
- (28) Adams, V. H.; McBryant, S. J.; Wade, P. A.; Woodcock, C. L.; Hansen, J. C. Intrinsic disorder and autonomous domain function in the multifunctional nuclear protein, MeCP2. *J. Biol. Chem.* **2007**, *282* (20), 15057–15064.
- (29) Garcia-Ortega, L.; De los Rios, V.; Martinez-Ruiz, A.; Onaderra, M.; Lacadena, J.; Martinez del Pozo, A.; Gavilanes, J. G. Anomalous electrophoretic behavior of a very acidic protein: ribonuclease U2. *Electrophoresis* **2005**, *26* (18), 3407–3413.
- (30) Leblond, C. P.; Clermont, Y. Definition of stages of the cycle of the seminiferous epithelium in the rat. *Ann. N.Y. Acad. Sci.* **1952**, *55*, 548–573.
- (31) Medzihradzky, K. F.; Darula, Z.; Perlson, E.; Fainzilber, M.; Chalkley, R. J.; Ball, H.; Greenbaum, D.; Bogyo, M.; Tyson, D. R.; Bradshaw, R. A.; Burlingame, A. L. O-sulfonation of serine and threonine: mass spectrometric detection and characterization of a new posttranslational modification in diverse proteins throughout the eukaryotes. *Mol. Cell. Proteomics* **2004**, *3* (5), 429–440.
- (32) Uversky, V. N.; Gillespie, J. R.; Fink, A. L. Why are “natively unfolded” proteins unstructured under physiologic conditions. *Proteins* **2000**, *41* (3), 415–427.
- (33) Fontana, A.; Zambonin, M.; Polverino de Laureto, P.; De Filippis, V.; Clementi, A.; Scaramella, E. Probing the conformational state of apomyoglobin by limited proteolysis. *J. Mol. Biol.* **1997**, *266* (2), 223–230.
- (34) Dunker, A. K.; Lawson, J. D.; Brown, C. J.; Williams, R. M.; Romero, P.; Oh, J. S.; Oldfield, C. J.; Campen, A. M.; Ratliff, C. M.; Hipp, K. W.; Ausio, J.; Nissen, M. S.; Reeves, R.; Kang, C.; Kissinger, C. R.; Bailey, R. W.; Griswold, M. D.; Chiu, W.; Garner, E. C.; Obradovic, Z. Intrinsically disordered protein. *J. Mol. Graphics Modell.* **2001**, *19* (1), 26–59.
- (35) Daughdrill, G. W.; Pielak, G. J.; Uversky, V. N.; Cortese, M. S.; Dunker, A. K. Natively disordered proteins. *The Protein Folding Handbook*; Kiehaber, T., Ed.; Wiley-VCH: Weinheim, 2004; pp 275–357.
- (36) Kawasaki, K.; Weiss, K. M. Evolutionary genetics of vertebrate tissue mineralization: the origin and evolution of the secretory calcium-binding phosphoprotein family. *J. Exp. Zool., Part B* **2006**, *306* (3), 295–316.
- (37) Kawasaki, K.; Weiss, K. M. Mineralized tissue and vertebrate evolution: the secretory calcium-binding phosphoprotein gene cluster. *Proc. Natl. Acad. Sci. U.S.A.* **2003**, *100* (7), 4060–4065.
- (38) Huq, N. L.; Cross, K. J.; Ung, M.; Reynolds, E. C. A review of protein structure and gene organisation for proteins associated with mineralised tissue and calcium phosphate stabilisation encoded on human chromosome 4. *Arch. Oral Biol.* **2005**, *50* (7), 599–609.
- (39) Sawyer, L.; Holt, C. The secondary structure of milk proteins and their biological function. *J. Dairy Sci.* **1993**, *76* (10), 3062–3078.
- (40) Loomis, R. E.; Bergey, E. J.; Levine, M. J.; Tabak, L. A. Circular dichroism and fluorescence spectroscopic analyses of a proline-rich glycoprotein from human parotid saliva. *Int. J. Pept. Protein Res.* **1985**, *26* (6), 621–629.
- (41) McClintock, T. S.; Glasser, C. E.; Bose, S. C.; Bergman, D. A. Tissue expression patterns identify mouse cilia genes. *Physiol. Genomics* **2008**, *32* (2), 198–206.
- (42) Spehr, M.; Schwane, K.; Riffell, J. A.; Zimmer, R. K.; Hatt, H. Odorant receptors and olfactory-like signaling mechanisms in mammalian sperm. *Mol. Cell. Endocrinol.* **2006**, *250* (1–2), 128–136.
- (43) Chalmel, F.; Rolland, A. D.; Niederhauser-Wiederkehr, C.; Chung, S. S.; Demougin, P.; Gattiker, A.; Moore, J.; Patard, J. J.; Wolgemuth, D. J.; Jegou, B.; Primig, M. The conserved transcriptome in human and rodent male gametogenesis. *Proc. Natl. Acad. Sci. U.S.A.* **2007**, *104* (20), 8346–8351.
- (44) Kleene, K. C. Patterns of translational regulation in the mammalian testis. *Mol. Reprod. Dev.* **1996**, *43* (2), 268–281.
- (45) Driscoll, J.; Zuo, Y.; Xu, T.; Choi, J. R.; Troxler, R. F.; Oppenheim, F. G. Functional comparison of native and recombinant human salivary histatin 1. *J. Dent. Res.* **1995**, *74* (12), 1837–1844.
- (46) Lasa-Benito, M.; Marin, O.; Meggio, F.; Pinna, L. A. Golgi apparatus mammary gland casein kinase: monitoring by a specific peptide substrate and definition of specificity determinants. *FEBS Lett.* **1996**, *382* (1–2), 149–152.
- (47) Medzihradzky, K. F.; Guan, S.; Maltby, D. A.; Burlingame, A. L. Sulfopeptide fragmentation in electron-capture and electron-transfer dissociation. *J. Am. Soc. Mass Spectrom.* **2007**, *18* (9), 1617–1624.
- (48) Xu, X.; Toselli, P. A.; Russell, L. D.; Seldin, D. C. Globozoospermia in mice lacking the casein kinase II alpha' catalytic subunit. *Nat. Genet.* **1999**, *23* (1), 118–121.
- (49) Escalier, D.; Silvius, D.; Xu, X. Spermatogenesis of mice lacking CK2alpha': failure of germ cell survival and characteristic modifications of the spermatid nucleus. *Mol. Reprod. Dev.* **2003**, *66* (2), 190–201.
- (50) Gifford, J. L.; Walsh, M. P.; Vogel, H. J. Structures and metal-ion-binding properties of the Ca<sup>2+</sup>-binding helix-loop-helix EF-hand motifs. *Biochem. J.* **2007**, *405* (2), 199–221.
- (51) Shin, D. W.; Ma, J.; Kim, D. H. The asp-rich region at the carboxyl-terminus of calsequestrin binds to Ca(2+) and interacts with triadin. *FEBS Lett.* **2000**, *486* (2), 178–182.
- (52) Publicover, S. J.; Giojalas, L. C.; Teves, M. E.; de Oliveira, G. S.; Garcia, A. A.; Barratt, C. L.; Harper, C. V. Ca<sup>2+</sup> signalling in the control of motility and guidance in mammalian sperm. *Front. Biosci.* **2008**, *13*, 5623–5637.
- (53) Ravindranath, N.; Papadopoulos, V.; Vornberger, W.; Zitzmann, D.; Dym, M. Ultrastructural distribution of calcium in the rat testis. *Biol. Reprod.* **1994**, *51* (1), 50–62.
- (54) Dym, M.; Clermont, Y. Role of spermatogonia in the repair of the seminiferous epithelium following X-irradiation of the rat testis. *Am. J. Anat.* **1970**, *128* (3), 265–282.

PR900082M